Pharm Res (2013) 30:2445–2458
DOI 10.1007/s11095-013-0982-y

EXPERT REVIEW

Magnetic Nanoparticles for Tumor Imaging and Therapy: A So-Called Theranostic System

Huining He • Allan David • Beata Chertok • Adam Cole • Kyuri Lee • Jian Zhang • Jianxin Wang • Yongzhuo Huang • Victor C. Yang

Received: 27 August 2012 / Accepted: 7 January 2013 / Published online: 24 January 2013

ABSTRACT In this review, we discussed the establishment of a so-called "theranostic" system by instituting the basic principles including the use of: [1] magnetic iron oxide nanoparticles (MION)-based drug carrier; [2] intra-arterial (I.A.) magnetic targeting; [3] macromolecular drugs with unmatched therapeutic potency and a repetitive reaction mechanism; [4] cell-penetrating peptide-mediated cellular drug uptake; and [5] heparin/protamine-regulated prodrug protection and tumor-specific drug re-activation into one single drug delivery system to overcome all possible obstacles, thereby achieving a potentially non-invasive, magnetic resonance imaging-guided, clinically enabled yet minimally toxic brain tumor drug therapy. By applying a topography-optimized I.A. magnetic targeting to dodge rapid organ clearance of the carrier during its first passage into the circulation, tumor capture of MION was enriched by >350 folds over that by conventional passive enhanced permeability and retention targeting. By adopting the prodrug strategy, we observed by far the first experimental success in a rat model of delivering micro-gram quantity of the large β-galactosidase model protein selectively into a brain tumor but not to the ipsi- or contra-lateral normal brain regions. With the therapeutic regimens of most toxin/siRNA drugs to fully (>99.9%) eradicate a tumor being in the nano-molar range, the prospects of reaching this threshold become practically accomplishable.

KEY WORDS brain tumor/cancer · cell-penetrating peptide · magnetic nanoparticles · theranostic system · tumor imaging and therapy

ABBREVIATIONS

ADEPT	antibody-directed enzyme prodrug therapy
ATTEMPTS	antibody targeted, triggered, electrically modified prodrug type strategy
BBB	blood–brain barrier
CPP	cell-penetrating peptide
DDS	drug delivery system
EPR	enhanced permeability and retention
ESR	electron spin resonance
GE	gradient echo
I.A.	intra-arterial
I.V.	intravenous
LMWP	low molecular weight protamine
MION	magnetic iron oxide nanoparticles
MRI	magnetic resonance imaging
PEI	polyethyleneimine
β-Gal	β-galactosidase
RES	reticuloendothelial system

H. He
School of Chemical Engineering and Technology, Tianjin University
Tianjin 300072, China

A. David • B. Chertok • A. Cole • K. Lee • J. Zhang • V. C. Yang (✉)
Department of Pharmaceutical Sciences, College of Pharmacy
University of Michigan, Ann Arbor, Michigan 48109-1065, USA
e-mail: vcyang@umich.edu

J. Wang • Y. Huang
Department of Pharmaceutics, School of Pharmacy, Fudan University
Shanghai, China

J. Wang • Y. Huang
Key Lab of Smart Drug Delivery, Ministry of Education and PLA
Shanghai 201203, China

Y. Huang
Shanghai Institute of Materia Medica, Chinese Academy of Sciences
501 Hai-ke Road
Shanghai 201203, China

H. He • V. C. Yang
Tianjin Key Laboratory on Technologies Enabling Development of Clinical Therapeutics and Diagnostics, School of Pharmacy
Tianjin Medical University, Tianjin 300070, China

INTRODUCTION

In the US alone, new brain tumors develop in nearly 2,000 children and 40,000 adults each year (1). Most brain tumors are primary, meaning that they rarely spread beyond the brain, as opposed to metastasic. Nearly 15–35% of brain tumors belong to glioblastoma multiforme, the most aggressive malignant brain tumor with average survival of less than 1 year after diagnosis, even with extensive treatments including surgery, radiation and chemotherapy (1–4). More adults die each year of brain tumors than of Hodgkin's disease or multiple sclerosis (5). Treatment of brain tumor faces a unique challenge comparing to other cancer types, because not only brain tissue is protected externally by the skull, which constrains the volume and regulates intracranial tissue pressure (6), but also are embedded deeply within an organ which carries a multitude of vital functions. Hence, even a benign brain tumor can be life-threatening and has to be removed, if it is in an area of the brain where it compresses structures that control critical body functions such as breathing or blood circulation. Treatment normally begins with surgery and is then followed with radiation and/or chemotherapy (7,8). However, when surgeons take out tumors elsewhere, they usually cut away some of the normal surrounding tissue for added assurance that all harmful cells have been removed. In the brain, removing extra tissue is not a ready option, since brain cells carry out specific, vital functions. Radiation can harm normal tissues that are near the treatment pathways (9–11). Indeed, the use of radiation on children under the age of 3 is often prohibited, because this is a critical time period of brain development (12). Chemotherapy has been offering very limited applications, primarily attributed to the palliative response and induction of systemic toxic effects due to lack of tumor selectivity of the drugs (13). Hence, the need of developing a non-invasive, clinically effective drug therapy in managing brain tumors is both acute and imperative, and the quest for such a system is of the greatest urgency.

Developing such a brain drug delivery system (DDS) faces a host of challenges, which had been described in some review articles (14–17). In general, limitations can be largely linked to five areas including: [1] skull protection and lack of targeting specificity for brain tumors; [2] low tumor accumulation of the drug carrier due to their rapid clearance; [3] lack of therapeutic potency for existing drugs; [4] impermeability of tumor membrane to drug uptake; and [5] drug-induced toxic effects on normal tissues.

Herein we illustrate an innovative system that can synchronize magnetic resonance imaging (MRI) with drug therapy for treatment of brain tumors.

THE DRUG DELIVERY SYSTEM ADDRESSING FIVE CHALLENGES

Proposed herein is a novel brain DDS that is capable of synchronizing MRI with brain tumor drug therapy. It integrates existing state-of-art technologies including [1] magnetic iron oxide nanoparticles (MION)-based drug carrier; [2] intra-arterial (I.A.) magnetic targeting; [3] macromolecular drugs (e.g. toxins) with unmatched therapeutic potency and a repetitive reaction mechanism; [4] cell-penetrating peptide (CPP)-mediated cellular drug uptake; and [5] heparin/protamine-regulated prodrug protection and tumor-specific drug re-activation into a single platform to prevail over each and all of the indentified challenges in achieving a non-invasive, MRI-visualized, highly efficacious yet safe brain tumor drug therapy with least drug-associated toxic effects.

As illustrated in Fig. 1, the system utilize MIONs as the drug carrier and a magnetic field around the head as the tool to achieve specific and selective brain tumor imaging and targeting. A macromolecular compound such as protein toxins or siRNA will be selected as the drug candidate (18,19). The drug will be chemically linked through a cytosol-degradable S-S bond to low molecular weight protamine (LMWP), a proven non-toxic yet potent CPP (20–25). On the other hand, the MION carrier possessing superparamagnetic behavior and a large magnetic core structure with superior magnetophoretic mobility will be synthesized and then coated with a biocompatible heparin-dextran polymer. The LMWP-modified drug (LMWP-Drug) and the heparin-coated MION (Hep-MION) automatically group into a nano-scale complex *via* electrostatic interaction between the positively charged LMWP and negatively charged heparin. Following self-assembly, the LMWP-Drug/Hep-MION complexes would display a unique prodrug feature during tumor targeting, due to inhibition of the cell-penetrating function of LMWP by heparin binding (26,27). To bypass the first-pass organ clearance thereby maximizing MION accumulation at the brain tumor, the drug-loaded MION carriers will be administered through a carotid catheter. Optimized magnetic field topography and a MRI-guided procedure to align the tumor lesion of the testing animal with the region of the maximal magnetic flux density, which has been successfully established previously (28), will be followed to abort possible embolism of afferent arterial vasculature due to I.A. injection as well as to maximize the selectivity of brain tumor targeting. After accumulation of the MION carriers at the interstitium of the tumor by both the EPR-mediated passive and magnetic-induced active tumor targeting, a rapid and on-command release of LMWP-Drug from the Hep-MION carriers will be triggered by administration of protamine, a clinical heparin antidote (29) that binds heparin stronger than LMWP (30). Although it has been reported that I.A. administered protamine can cross blood–brain barrier (BBB) and reach the brain parenchyma (31), protamine is given *via* the nasal route to

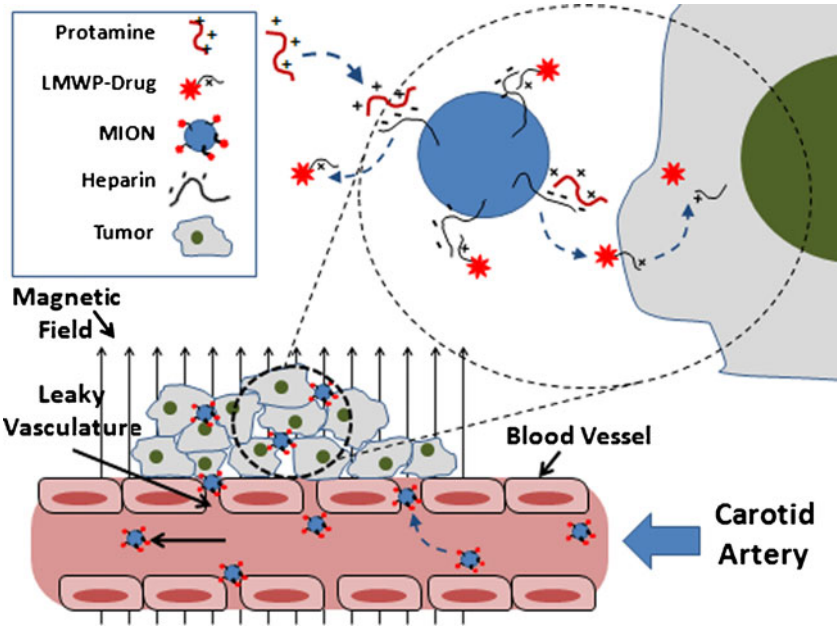

Fig. 1 Schematic illustration of the proposed brain drug delivery.

achieve the highest efficacy and safety. Preliminary results (data not shown) reveal that nasal route can lead to a rapid transportation of a sufficient amount of protamine into the brain for this triggering purpose. Taking advantage of our early findings that MION are cleared quickly (~5 min) from circulation (also from the normal brain) but retained for several hours in the tumor due to post-effect of magnetic targeting (32), protamine will be administered immediately after significant MION accumulation in the tumor is verified with MRI, thereby enabling the drug-induced toxic effect caused by non-specific uptake of the released but unmasked LMWP-Drug to be attenuated. Once inside the tumor cells by the LMWP-mediated internalization process, the drug is detached from LMWP *via* degradation of the S-S bond by the presence of elevated glutathione and reductase activity in the cytosol (33,34), initiating tumor apoptosis. Due to its cell-impermeable nature, the cytosol-delivered macromolecular drug would not be affected by the multi drug resistance effect. Overall, the proposed brain tumor drug therapy should be both safe and non-toxic, because only a negligible amount of unmasked LMWP-Drug would be present in circulation after protamine administration to interact with normal tissues, due to the short plasma half-life of MION.

Reviewed below are our previous findings that provide solutions to all the five challenges (Table I) and also a proof-of-concept demonstration of the general feasibility of this DDS.

SOLUTION TO CHALLANGE 1: APPLICATION OF MION AND MAGNETIC TARGETING

Unlike other organs, the brain is encased in the skull that protects it from outside forces. The hard-built bone structure of the skull renders the brain least accessible to drug delivery *via* direct injection methods. Application of MION as the drug carrier for tumor targeting is thus an appealing strategy in resolving the skull barrier because, with the aid of an external magnetic field, this approach could deliver drugs to any site of choice. In addition, it was shown that MION could penetrate through the tumor capillary endothelium *via* the enhanced permeability and retention (EPR) effect (35), which means certain sizes of molecules (typically liposomes, nanoparticles, and macromolecular drugs) tend to accumulate in tumor tissue much more than they do in normal tissues. To take the full benefit of the EPR effect for tumor targeting, MION should be controlled within the size range of 100–300 nm. It has been reported that particles >300 nm will be subjected to hepatic and reticuloendothelial system (RES) clearance, whereas <10 nm will be cleared by renal filtration. Applying an external magnetic field would not only upgrade this EPR *passive* targeting to an *active* magnetic targeting, but also provides a magnetic-enhanced retention of MION once they are captured in the tumor interstitium. Added to tumor targeting is an even more attractive clinical feature for MION. As noted, MION is an enhancer of proton spin-spin *(T2/T*2)* relaxation, and thus the reduction in signal intensity due to their accumulation could render the effects of drug therapy being non-invasively monitored *via* the use of clinical MRI.

Visualization of Brian Tumor Targeting *via* MRI

To examine the benefits of utilizing MION as the drug carrier in achieving magnetic-mediated active targeting and MRI visibility of the brain tumor, starch-coated MION (branch name: G-100) was injected *via* the tail vein into the

Table I Summary of Challenges to Brain Drug Delivery Systems, Solutions and Related Publications

No.	Challenges	Solutions	Related publications
1	Skull protection and lack of targeting specificity for brain tumors	Application of MION and magnetic targeting	Biomaterials. 2008;29(4):487–496 J Control Release. 2008;132(3):e61-e62 Mol Pharm. 2009;7(2):375–385
2	Low tumor accumulation of the drug carrier due to their rapid clearance	Magnetic targeting *via* intra-arterial (I.A.) administration	J Control Release. 2011;155(3):393–399 Biomaterials. 2011;32(26):6245–6253
3	Lack of therapeutic potency for existing drugs	Application of macromolecular drugs with unmatched therapeutic potency	Biomaterials. 2010;31(24):6317–6324
4	Impermeability of tumor membrane to drug uptake	Application of CPP-mediated cellular drug uptake	AAPS J. 2001;3(3):7–14 AAPS J. 2001;3(3):15–23 AAPS J. 2001;3(3):24–31 Faseb J. 2005;19(11):1555–1557 Thromb Res. 1999;94(1):53–61 Biochemistry (Moscow). 2003;68(1):116–120 J Gene Med. 2003;5(8):700–711
5	Drug-induced toxic effects on normal tissues	Application of heparin/protamine-regulated prodrug protection and tumor-specific drug re-activation	Expert Opin. Drug Deliv. 2008;5(11):1255–1266 Curr Pharm Design. 2010;16(21):2369–237658 J Control Release. 2002;78(1–3):67–79 Curr Pharm Design. 2010;16(21):2369–2376

glioma-bearing rats and then subjected to experiments (36). Figure 2 presents a subset of a typical series of MRI images obtained from (a) magnetically targeted; and (b) non-magnetically targeted animals before and after intravenous (I.V.) injection of MION. The brain tumors were clearly visible on the baseline T2-weighted images in both animal groups. As seen in Fig. 2a, the gradient echo (GE) images of the targeted animal acquired 1 and 3 h post injection (0.5 and 2.5 h post magnetic targeting, respectively) exhibited a region of pronounced hypo-intensity compared to the baseline GE image. This hypo-intense region indicated the presence of magnetic nanoparticles within the tumor tissue. In contrast, the post-injection images of the non-targeted animal (Fig. 2b) displayed no detectable signal reduction within the glioma lesion. These results indicated that MION accumulation in the tumor by conventional passive targeting *via* EPR was nearly negligible. However, with use of magnetic targeting, both the accumulation and retention of MION in the tumor were vastly improved to a degree that was clearly visible by MRI.

Quantification of MION Accumulation by MRI

To quantitatively determine MION accumulation in the brain, we developed an innovative technique that would allow inferring information from R2 relaxivity maps of the animals, assuming that the change in relaxivity relative to the pre-scan (dR2) would be dictated by the change in MION concentration (32). Briefly, the R2 values used to analyze the time course of R2 relaxivity change after MION administration were obtained from the mean signal intensity within the defined regions of interest (ROI; manually drawn in the tumor lesion and contralateral normal brain) on the R2 relaxivity maps. The change in R2 relaxivity caused by the presence of the contrast agent (i.e. MION) within the tissue of interest at time t (i.e. dR2(%)), expressed as percentage change of the initial (pre-scan; $t=0$) relaxivity value according to the equation :

$$dR2(\%) = \frac{R2(t) - R2(0)}{R2(0)} \times 100\% \quad (1)$$

would correlate to MION concentration in the tissue at the specific time t. To verify our results, dR2 changes measured *in vivo* using MRI were compared to MION concentrations precisely quantified *ex vivo* by using the electron spin resonance (ESR) method. As known, ESR has been used widely to directly quantify the presence of paramagnetic species (37–39). As shown in Fig. 3, the ESR results obtained from the excised tumors were found to be linearly correlated (slope=0.57 g tissue/n-mol Fe, $p=0.0001$, $R2=0.88$) with the dR2 data acquired from the MRI image map.

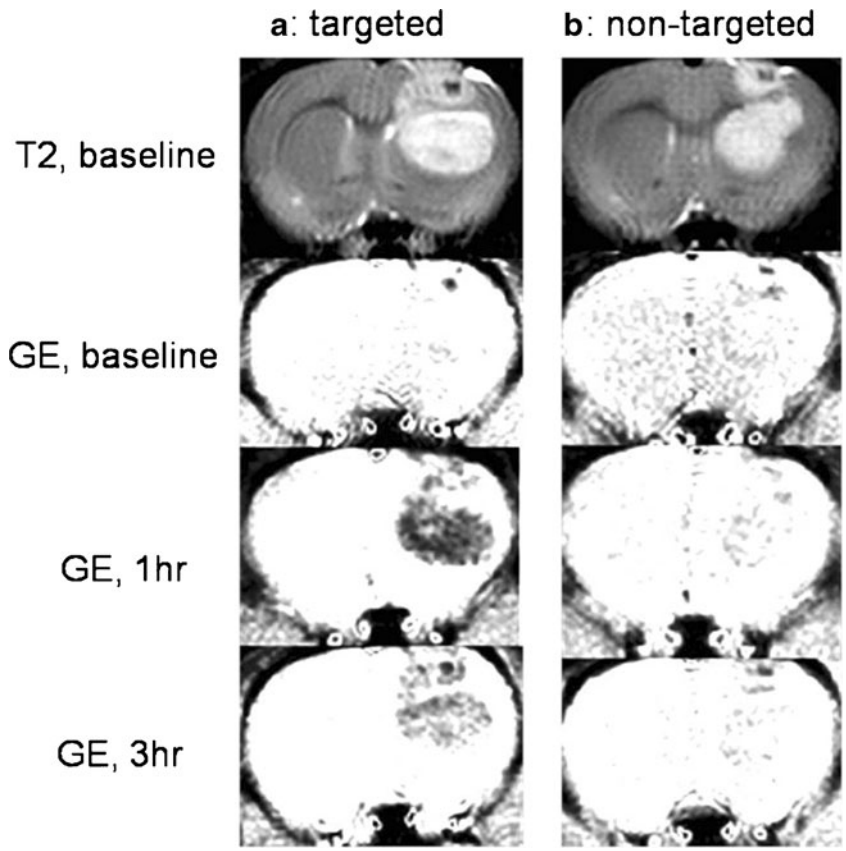

Fig. 2 MRI scans showing MION accumulation in 9 L gliosarcoma (**a**) with; (**b**) without magnetic targeting. Reprinted with permission from (32).

Targeting Efficiency and Selectivity *via* Intravenous (I.V.) Administration

Figure 4 shows that MION concentrations determined by ESR showed that i.v. administration along with magnetic targeting resulted in 11.5-fold increase ($p<0.0005$) in MION accumulation in tumors with magnetic targeting (Column #1 from left; 29.8±7.9 nmol Fe/g tissue) over that of the tumors without magnetic targeting (Column #2 from left; 2.6±0.7 nmol Fe/g tissue); indicating a markedly enhanced efficiency in capture and retention of MION by the tumor *via* application of an external magnetic field. Equally important was the finding of a 9.5-fold difference ($p<0.0005$) in the MION concentration between the tumors (29.8±7.9 nmol Fe/g tissue; Column #1) and contralateral normal brain (3.1±2.1 nmol Fe/g tissue; Column #3 from left) of animals with magnetic targeting, suggesting a greatly distinct targeting selectivity on brain tumor over the contra-lateral normal brain. On the other hand, the marginal difference in MION accumulation between tumors and normal brain tissues of the animals without magnetic targeting (2.6±1.4 *vs.* 0.5±0.1 nmol Fe/g tissue; Column #2 from left *vs.* Column #4) indicated that contribution of the EPR effect to tumor retention of MION by

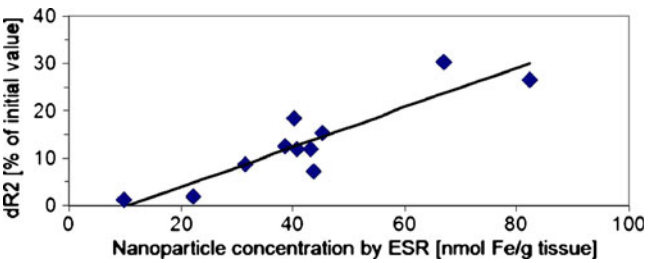

Fig. 3 Plot showing linear correlation between the MRI-derived dR2 and ESR-determined MION quantity in excised tissue samples.

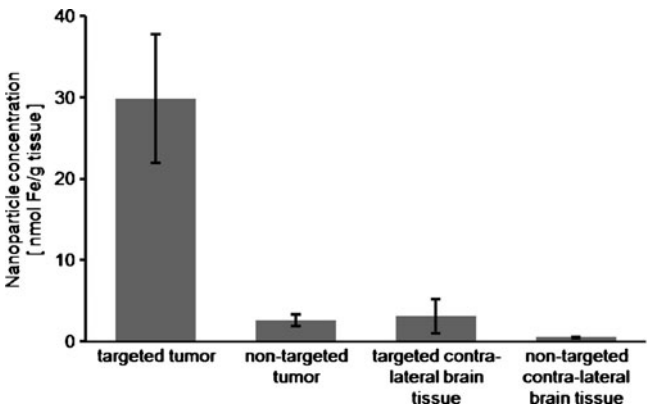

Fig. 4 MION concentration in excised tumor and contra-lateral brain tissues quantified by ESR spectroscopy. Data expressed as Mean ± SE. $n=6$. Reprinted with permission from (32).

passive targeting was relatively minimal, despite the pronounced differences in vascular permeability between the intact BBB and the compromised blood tumor barrier.

SOLUTION TO CHALLANGE 2: MAGNETIC TARGETING *VIA* INTRA-ARTERIAL (I.A.) ADMINISTRATION

Despite the 11.5-fold increase in the total glioma exposure to MION by magnetic targeting over the non-targeted tumor tissues, the overall MION accumulation in the tumor (i.e. ~30 nmol Fe/g tissue) was still below 0.01% of the initially administered dose (12 mg Fe/ kg); a finding consistent with that documented in the literature (40,41). This was primarily due to rapid renal and hepatic clearance of MION, particularly of those with positive charges. It was reported that polylysine-coated MION had a plasma half-life of merely 1–2 min (42). I.A. administration offers the advantage of allowing carriers to bypass renal and hepatic clearance during their first passage through the circulation, and was therefore exploited to further enhance brain tumor magnetic targeting. It should be pointed out that with recent advances in endovascular technology and the increased safety of angiographic procedures, carotid administration of nanoparticles has become a clinically-relevant alternative to I.V. injection (43).

Nonetheless, achieving a high first-pass nanoparticle concentration with intra-carotid administration can also present a serious pitfall in conjunction with magnetic targeting. Consistent with findings by other investigators (43), we discovered that when mice were injected with high concentrations of MION, significant embolism of the afferent vasculature occurred due to their aggregation (see results later). Occlusion of the carotid artery, which directly supplies the normal brain parenchyma, can lead to severe neuro-sequelae (44) and must thus be avoided. Also, blockage of the blood flow would hinder the convective transport of MION towards the tumor site. Magnetic field topography and strength have been shown the capability in modulating the extent of MION aggregation at arterial and capillary blood flow rates (45), and could therefore offer a creative solution to this dilemma.

Based on the assumption that arterial deposition of MION could be avoided by preserving the intact flow dynamics in the injected artery and minimizing the magnetic flux density away from the target site, we designed a novel magnetic targeting strategy by optimizing the arterial flow dynamics and magnetic field topography to override the vascular embolism obstacle (46). To maintain carotid flow dynamics, we employed a new catheterization procedure that would not require vessel occlusion, by inserting a thin silica capillary tubing (OD: 150 μm), which functioned as a needle, through the vascular wall without compromising the integrity of the artery. This new catheterization technique did not impede the blood flow through the artery, and allowed infusion of MION suspension at a rate of 5 μL/s, while maintaining intact arterial hydrodynamics.

Our innovative and new magnetic targeting approach (28) involved mounting of a small cylindrical permanent magnet (d=9 mm) to a tapered pole of a standard (Fig. 5a) dipole electromagnet, as illustrated in Fig. 5b. This configuration served to divert the magnetic flux lines emanating from the electromagnet poles to pass through the low resistance cylindrical attachment, thus generating a local maximum of the magnetic field on the exposed pole face of the cylinder. Mapping of the magnetic flux density revealed that the dipole electromagnet, used previously in our targeting studies, generated broad-range and shallow-gradient topography (Fig. 5c). In contrast, the topographic map obtained with the optimized magnet configuration (Fig. 5d) exhibited a focal region of maximal flux density (350 mT) which decayed rapidly with the distance from the peak. It is also noteworthy that the small dimensions of the cylindrical attachment allowed to focus the magnetic flux density over a narrow circular region (d~5 mm) approximating to the cross-section of the tumor lesion. As seen in Fig. 5f, by applying this magnetic setup with optimized magnetic field topography, we achieved a 6-fold reduction of the magnetic force at the injection site, alleviating MION aggregation in the afferent vasculature seen previously in Fig. 5e, under an intact carotid blood flow condition.

To fully utilize the benefits of the magnetic field topography, our next step was to align the tumor lesion with the region of the maximal magnetic flux density by properly positioning the rat with respect to the magnetic setup. For such positioning, we used MRI to determine the intracerebral localization of the tumor lesion, since the tumor could be clearly visualized as a hyperintense region on T_2-weighted MRI scans. To assess the effects of the new approach on targeting efficacy, experiments were conducted using both I.V. and I.A. injection of polyethyleneimine (PEI)-coated MION (PEI-MION) since with its highly positive surface change (47), the plasma clearance of PEI-MION was found to be 80-fold faster than that of starch-coated MION (i.e. G100) (data not shown). Such an exceedingly short plasma half-life of PEI-MION rendered the beneficial effects of I.A. magnetic targeting over the I.V. method to be magnified and clearly verified. As anticipated, while animals with i.v. magnetic targeting did not show any discerned difference between the post-targeting and the baseline GE scans due to rapid systemic clearance of PEI-MION (Fig. 6a), animals with I.A. targeting displayed a pronounced hypointense region in the post-targeting GE scans corresponding to significant MION accumulation in the tumor. Quantification of MION accumulation in excised tumors revealed a 30-fold

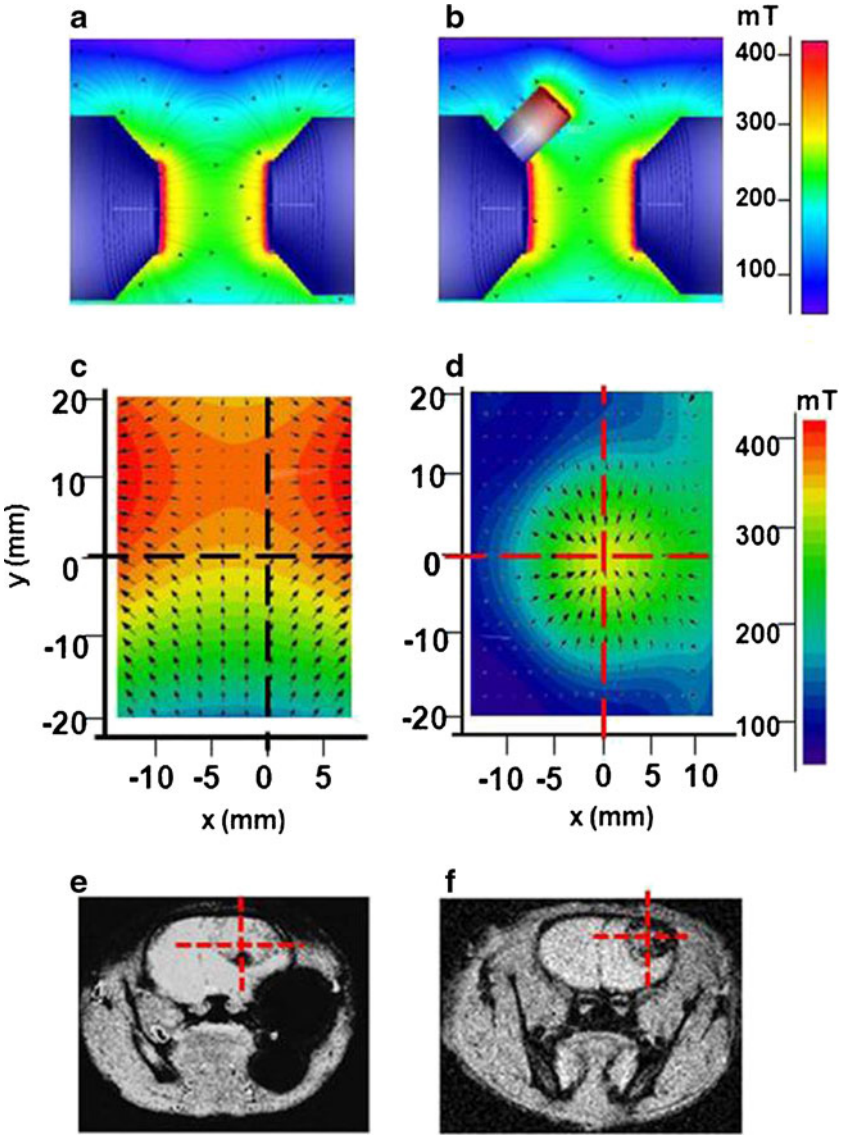

Fig. 5 Models of (**a**) original; (**b**) modified magnetic configurations with (**c** and **d**) of their respective topographic maps generated by the implemented magnetic setups. Typical axial MRI scans of the rat head acquired after magnetic targeting with (**e**) original and (**f**) modified magnetic setups. Reprinted with permission from (28).

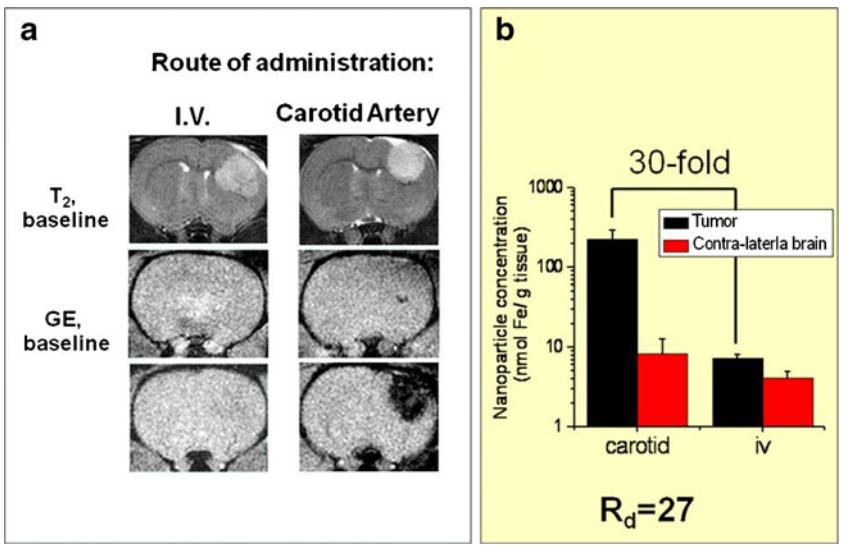

Fig. 6 (**a**) MRI head-scans of 9 L-glioma bearing rats of: *Left*: intravenous (I.V.) and *Right*: carotid artery magnetic targeting; and (**b**) MION accumulation in tumor and contra- lateral brain tissues was measured by ESR; following I.V. and I.A. injection of PEI-MION32. Reprinted with permission from (47).

increase in tumor capture of PEI-MION by I.A. over I.V. injection (Fig. 6b, 222.8 ±66.7 *vs.* 7.3±0.8 nmol Fe/g tissue, respectively). Interestingly, there was also significant difference in targeting selectivity on brain tumor over contra-lateral normal brain (222.8±66.7 *vs.* 8.6±1.0 nmol Fe/g tissue) when comparing the two columns on the left of Fig. 6b following I.A. injection.

It should be pointed out that our results of tumor accumulation of 0.5% of the originally administered MION dose were by far the highest MION capture by a brain tumor reported in the literature under clinically relevant conditions. Although in 1998 Pulfer and Gallo (48) reported an unrealistically high MION capture in rat glioma *via* I.A. targeting, their results were obtained under permanent ligation of all of the other arteries; an unacceptable procedure in clinical practice. There was also no follow-up from these, or other, investigators to further confirm such findings since 1998.

SOLUTION TO CHANLLANGE 3 AND 4: APPLICATION OF MACROMOLECULAR DRUGS AND CELL PENETRATING PEPTIDE

Most of existing drugs are small, hydrophobic compounds that exert cytotoxic actions by inhibiting DNA synthesis or causing irreparable damage to existing DNA. Action of such agents therefore follows a *suicidal* mechanism, meaning that they only can act *once* with their substrates. Small cytotoxic drugs also localize more efficiently in normal tissues than in tumors, due to the high interstitial pressure and unfavorable blood flow within rapidly growing tumors. Because of these limitations, drug concentrations accumulated at the brain tumor are usually extremely low (<1% of the injected dose), rendering most existing small molecule drugs ineffective clinically. To address this low potency issue for existing drugs, we exercised the novel strategy of utilizing macromolecular drugs (e.g. toxins, siRNA) with superior efficiency and a *repetitive* reaction mechanism to supersede the potency barrier by eradicating tumor at exceedingly low bioavailable drug concentrations at the target site. For instance, IC_{50} of the proposed gelonin against human glioma cells was shown to be 15 pmol (49), about 7 orders of magnitude lower than that of commonly used anti-glioma agent BCNU (130 μM) (50).

Membrane of tumor cells and virtually of all cell types is permeable to only small (<700 Da), hydrophobic drugs. Although a variety of means such as microinjection, scrape loading, and electroporation have been exploited to deliver protein drugs into living cells (51,52), these methods are inefficient and also not suitable for clinical use. The most widely used method to-date is *via* the receptor-mediated endocytosis (53). This cell-entry method, however, requires invagination and vasculation of the membrane lipid bilayer to form free cytoplasmic vesicles. Since large drugs such as proteins that have entered this pathway remain enclosed within the lipid vesicles, they do not have access to the cell cytoplasm; a pre-requisite for such drugs to exert cytotoxic effects. To counter this obstacle, we proposed a novel strategy by linking the macromolecular drug with a potent yet non-toxic CPP, LMWP (20–25). Animal studies demonstrated that by covalently linking CPP (e.g. TAT) to almost any type of drugs (e.g. proteins) or carriers (e.g. MION), CPP was able to ferry the attached cargos into all organ/-tissue types including the brain (54), without causing membrane perturbation or cytotoxicities (27,54).

The therapeutic prowess of protein drugs over small agent, and the success of utilizing CPP in overriding the membrane barrier and achieving cellular protein uptake have been addressed in our previous ATTEMPTS system in tumor treatment (30). As summarized in a recently published review (55), nmol quantity of TAT-gelonin was already sufficient to eradicate the tumor in a mouse CT-26 xenograph model.

We conducted pilot tumor regression studies on CT26 colon carcinoma-bearing BALB/c mice using TAT as the representative CPP and gelonin, a protein toxin that inhibits protein synthesis by cleaving mRNA but is also known to be cell-impermeable, as the model protein drug. As shown in Fig. 7, mice treated with TAT-gelonin (TAT-Gel) conjugate displayed remarkable regression in tumor growth compared to the gelonin alone and PBS control group. The average tumor weights after 4 weeks of treatment were 0.33+0.12 g (c and e: n=10), 2.86+0.5 g (b and d: n=9) and 3.16+0.65 g (a: n=5) respectively. The fact that micrograms (or nmol) of gelonin was already sufficient to eradicate the tumor showed

Fig. 7 Excised tumors from mice treated, from top to bottom, with: (**a**) PBS; (**b**, **d**) free gelonin (100 μg); (**c**, **e**) TAT-Gel (100 μg Gel equivalent). Reprinted with permission from (30).

the therapeutic prowess of protein drugs over small agents. These results also gave proof of using CPP to override the tumor membrane barrier.

SOLUTION TO CHANLLANGE 5: APPLICATION OF PRO-DRUG SYSTEM

Like most organs, the brain lacks a targeting specificity. Hence, any drug intended for combating the brain tumor, regardless how it is administered, would distribute profoundly to the other organs/tissues, resulting in limited therapeutic effects toward the tumor but toxic drug side effects toward non-targeted organs/tissues. Although the lack of tumor selectivity can be circumvented by attaching the drug with a targeting moiety such as an antibody or a peptide ligand (e.g. RDG), yet adding the targeting function alone would not completely abort the drug-induced side effects; simply because the drug could still exert cytotoxic effects on peripheral tissues along its travel to the target. Combining both the targeting and prodrug features into a single delivery system, in which the drug remains inactive during its travel and targeting but is then converted to the active form at the tumor site, deems to be a clever way to resolve this selectivity limitation. Indeed, based on this principle, an approach termed antibody-directed enzyme prodrug therapy (ADEPT) (56,57), which permits specific enzymatic conversion of a prod rug at the target site to the active parent drug, has attained some success in delivering small therapeutic agents to tumors without drug-induced toxic effects. Recently, another approach developed by our group termed antibody targeted, triggered, electrically modified prodrug type strategy (ATTEMPTS) (58), which invents the prod rug feature onto a protease drug (t-PA) by blocking the catalytic domain of the drug with an appended macromolecule and then reinstates the original proteolytic activity of the drug at the target site by releasing the blockage with a triggering agent, has further advanced the utility of this type of delivery approach to include macromolecular drugs. However, without a means to facilitate an effective cellular drug uptake, the ADEPT system is restricted to mainly existing small drugs (e.g. doxorubicin that can enter cells by itself (59)) and the ATTEMPTS system to enzyme drugs that exert activities solely in the circulation or extracellular environment (e.g. asparaginase (60)).

To prevail over this obstacle of drug-induced systemic toxicity, we devised a highly innovative prodrug strategy by incorporating a prodrug feature into a targeted DDS, so that the drug will remain inactive in the circulation during tumor targeting thus aborting its effect on normal tissues, but is then converted to its active form selectively at the tumor target, thereby causing destruction only to tumor cells. we utilized a heparin-induced inhibition on the cell-penetrating activity of CPP to create the prodrug feature, and subsequently the protamine-induced reversal of heparin inhibition to resume cell transduction of the protein drug *via* the CPP function (55).

In the same TAT-gelonin (TAT-Gel) system mentioned in Solution to 3 and 4 (Fig. 7), adding heparin to the TAT-Gel solution prior to its injection showed a complete inhibition on TAT-mediated gelonin uptake, as no statistically meaningful regression on tumor mass was observed (d: 2.86 + 0.57 g) when comparing with the control group (a: 3.16 + 0.65 g). Addition of protamine to the heparin-inhibited TAT-Gel, however, completely reversed this inhibition and resumed the cytotoxic activity of TAT-Gel, as tumor growth was reduced to an insignificant mass value of 0.17 + 0.09 g (e).

It should be pointed out that despite the promise of CPP in resolving the membrane barrier, the absence of selectivity by CPP in mediating cell entry renders this method an unacceptable practice in drug delivery, due to risk of introducing drug toxicity on normal organs/tissues (61). Our approach is the first known system to overcome this selectivity issue, enabling CPP-mediated cellular drug delivery to be practically applicable clinically.

PROOF OF CONCEPT DEMONSTRATION

To provide a proof-of-concept demonstration of the overall feasibility of our DDS, β-Galactosidase (β-Gal) was selected as the model protein drug during the initial study to verify the utility of the above strategy in selectively delivering active protein into the brain tumor; due to its large size (MW: 465 kDa) and easily detectable *in vivo* activity. Commercial heparin-linked MION (Hep-MION) from Chemicell was used as the drug carrier. β-Gal was modified with PEI for several reasons. First, PEI was known to possess the trans-cell activity similar to that of the CPPs adopted in our system. Uptake by brain tumors of PEI-modified magnetic carriers *via* an adsorptive endocytosis mechanism has already been documented (48,62). Indeed, both PEI and CPP have been widely used as an effective transfection agent to enhance cellular uptake of DNA (63,64). Furthermore, after electrostatic adsorption of the positively charged PEI-β-Gal onto the negatively charged Hep-MION, the self-assembled β-Gal/MION would carry a cationic surface similar to that of PEI-MION which was studied in our previous magnetic targeting work (47).

β−Gal was chemically modified with short-chain PEI (MW: 1200 Da) using a previously established EDC activation procedure (65). The PEI-β-Gal conjugates thus prepared retained >80% of original enzyme activity. They were then loaded onto Hep-MION *via* simple electrostatic

interaction between PEI and heparin. Results from ζ-potential measurements revealed that the surface of Hep-MION was converted from the initially negative value (−33 mV) to positive value (+24 mV) following complexation. Analysis of the protein content yielded a loading capacity of 7.2±0.4% (w/w), significantly higher than the previously reported loading of 2.8±0.16% of β-Gal on PLGA microspheres (66).

For magnetic targeting, Fisher 344 rats harboring 9 L brain glioma were placed supinely on the platform with head being positioned according to the mapped magnetic field topography described previously to align the tumor with the peak field density and gradient (28,46). The magnetic field density at the pole face of the magnet was adjusted to 0 T (control) or 350 mT (experimental). Animals were then injected with the PEI-β-Gal/Hep-MION complexes at a dose of 1.8 mg protein and 12 mg Fe/kg *via* catheterized carotid artery and retained in magnetic field for 30 min. Rats were imaged with MRI before nanoparticle administration and after the magnetic targeting as described earlier. Protamine was then administered nasally. Previous studies using nasal administration of FITC-labeled protamine to mice and then imaging the brain organs with a Xenogen IVIS instrument revealed that the fluorescence intensity in the olfactory bulb and brain of animals with nasal protamine was 10- and 2-fold stronger than the respective organs in the control animals (data not shown). Immediately following protamine administration, the rats were transcardially perfused with cold PBS, dissected, and the isolated brain divided into right and left hemispheres. The tumor was carefully separated from the normal tissue of the right hemisphere, and tumor segments were stored at −80°C for β-Gal histochemistry studies.

MRI scans showed consistent results as observed previously. To avoid redundancy and repetition, MRI scans will not be presented again. In general, in the absence of magnetic targeting, no clear difference was visually discerned between the post-targeting and the baseline GE brain scans of control animals receiving PEI-β-Gal/Hep-MION but without magnetic targeting. With magnetic targeting, the GE post-targeting scan of experimental animal again displayed a region of pronounced hypointensity, spatially corresponding to the location of the tumor lesion; validating a successful delivery of the β-Gal-loaded MION to the tumor site.

To further assess brain distribution and functionality of the delivered protein, we also analyzed the excised tumor and contra-lateral brain tissues for β-Gal activity. Again, no significant difference in activity ($p=0.596$) was observed between the tissues of control animals injected with the PEI-β-Gal/Hep-MION complexes but without magnetic targeting. In sharp contrast, tumors of magnetically-targeted rats exhibited significantly higher β-Gal activity ($p<0.001$) than the control tissues. In particular, a 4.7-fold higher β-Gal activity ($p<0.001$) was detected in tumors of the animals with magnetic targeting (636±42 μU/g tissue) than those without magnetic targeting (134±46 μU/g tissue), confirming viability of the developed magnetic targeting procedure for delivery of a functional protein to the target site. Moreover, in targeted animals a 7.5-fold higher selectivity of β-Gal localization in the brain tumor (636±42 μU/g tissue, $p<0.001$) than in the contra-lateral brain tissues (85±30 μU/g tissue).

The most convincing proof of the specific brain tumor delivery came from histochemical evaluation of β-Gal activity using X-Gal staining of various brain sections in targeted rats. As shown in Fig. 8, excessive deposition of β-Gal in the tumor (T; Left) but not the ipsi-lateral (IB, Middle) or contra-lateral (CB; Right) normal brain regions was observed, confirming tumor-selective β-Gal delivery due to release of PEI-β-Gal from Hep-MION at the tumor target by nasal protamine. Although at a higher magnification (inset) many β-Gal activities were seen to locate outside the capillaries (stained in red), this phenomenon could be due to an artifact resulting from non-homogeneous staining of the capillary. Future investigation is therefore warranted to fully confirm the location of the tumor-delivered β-Gal. These results represent by far the first experimental success in a rat model of delivering microgram quantity of the 465 kDa β-Gal selectively into a brain tumor but not to normal brain regions (46).

At this moment, the mechanism of β-Gal delivery into the tumor is not completely clear. Of course the most likely route would be through the PEI-mediated cell-internalization of the PEI-β-Gal conjugates which were released *via* the triggering action of nasal protamine. However, as discussed earlier, tumor uptake of PEI-modified magnetic carriers *via* adsorptive endocytosis has been reported (48,62), and thus it could also be that the entire PEI-β-Gal/Hep-MION complexes were delivered into the tumor due to presence of PEI-covered surfaces on the complexes. On the other hand, it was also documented in the literature (63,67) that ionic binding between PEI-modified compounds and heparin-modified carriers is reversible, and thus it could be that the PEI-β-Gal conjugates were desorbed from the Hep-MION carrier after a time span following tumor localization of the complexes by magnetic targeting. The desorbed PEI-β-Gal could then cross the vascular wall into the tumor interstitium *via* the adsorptive endocytosis mechanism demonstrated by those investigators. Our ESR analysis on the content of MION carrier and enzymatic assay on β-Gal activity of dissected tumor tissues yielded a lower MION/PEI-β-Gal ratio comparing to that of the original complex, implicating that both events might have occurred concurrently; although detailed investigations are warranted to further prove this aspect. Regardless, highly selective tumor targeting and successful tumor delivery of the very large β-Gal have been accomplished.

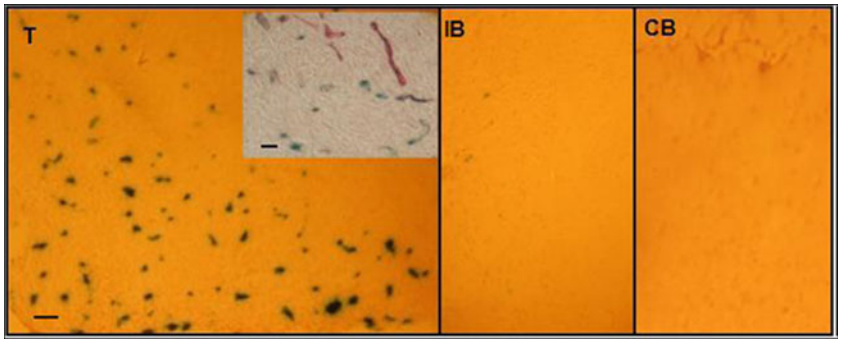

Fig. 8 Histochemical analysis of cryo-sections from (T) tumor (*left*); ipsilateral brain (*middle*); and (63) contralateral brain (*right*) regions (scale: 100 μm). Sections were stained with X-Gal. *Inset*: at higher magnitude (scale: 25 μm); capillaries stained with Burr-stone's Red.

To our knowledge, this is by far the first report that describes selective delivery of a significant amount of a macromolecular protein compound (aside from antibodies) directly into the parenchyma of a brain tumor but not in the normal brain regions. The only other report on successful brain delivery of β-Gal was from Dowdey's group with the focus on demonstrating the prowess of the cell-penetrating TAT peptide (a CPP) on its mediated cell protein transduction (54). In their report, 4 h after intraperitoneal injection into the mice of a fused protein consisting of TAT and a significantly shortened β-Gal monomer (MW: 120 kDa), the β-Gal activity was found in tissues of all organ types including the brain. Nevertheless, the absence of selectivity by CPP on its mediated cell internalization prohibits it from any possible clinical use in achieving effective brain tumor drug delivery, due to concerns of introducing drug-associated toxic effects (61). In addition, this method required administration of 40–200 nmol/kg of the TAT-β-Gal conjugates in order to achieve a detectable level of β-Gal in the brain, whereas our results indicated that we were able to achieve a higher β-Gal accumulation in the brain tumor with a dose as low as merely 4 nmol/kg (10 to 50-fold dose reduction), and yet without detection of β-Gal activity in the ipsilateral and contralateral normal brain regions. With integration of the potent cell-penetrating LMWP in replacing PEI to facilitate tumor uptake, further optimization of the efficacy of I.A. magnetic targeting using MION with superior magnetophoretic mobility incorporation of the reversible prodrug feature with heparin/protamine-induced regulation, and selection of a potent, tumor-specific macromolecular drug such as the recently reported tumor-specific ATF5-siRNA, the outcome of this proposed non-invasive DDS in treating brain tumors could be even more promising.

Toxicity, Pharmacokinetics, and Biodistribution Evaluation

As a key organ of the RES, the liver is a major depository for drug carriers including MION. Nevertheless, it is believed that the proposed DDS would not induce significant liver or systemic toxicity, since as a clinical contrast agent MION has been extensively evaluated in animal and preclinical settings and proven to be non-toxic (68), and thus the LMWP-Drug/MION complexes are expected to remain intact (i.e. prodrug) without releasing LMWP-Drug to trigger systemic toxicity. However, to ensure clinical safety of this DDS, comprehensive liver and systemic toxicity will be evaluated. Although the system will utilize the intra-arterial (I.A.) injection route, pharmacokinetics and biodistribution can actually be studied by intravenous injection. This is because after I.A. injection MION would rapidly join systemic circulation as if they were I.V. injected, providing the fraction of the MION dose entrapped in the brain on the first pass is rather small (69). Aside acquiring basic information, since our DDS proposes a triggered release of LMWP-Drug from the Hep-MION carrier, pharmacokinetic findings would be of great value to verify whether these two components could remain attached *in vivo* in the absence of protamine. Results of the will be reported in future publications.

CONCLUSIONS

In this review, we instituted basic principles including the use of: [1] MRI, [2] magnetic targeting, [3]macromolecular drugs, [4] CPP-mediated intracellular drug uptake, and [5] prodrug and tumor-specific drug activation into one single DDS to overcome all of the obstacles, thereby achieving a potentially non-invasive, MRI-guided, clinically enabled yet minimally toxic brain tumor drug therapy. Innovation of this system lies in its integration of state-of-art technologies and enabling them to function as a single unit to address each and collectively all of the scientific challenges for brain delivery systems.

By applying a topography-optimized I.A. magnetic targeting to dodge rapid organ clearance of the carrier during its first passage into the circulation, tumor capture of MION was enriched by >350 folds over that by conventional passive EPR targeting. Also by adopting the prodrug strategy,

we observed by far the first experimental success in a rat model of delivering micro-gram quantity of the large (465-kDa) β-Gal model protein selectively into a brain tumor but not to the ipsi- or contra-lateral normal brain regions. With the therapeutic regimens of most toxin/siRNA drugs to fully (>99.9%) eradicate a tumor being in the nano-molar range, the prospects of reaching this threshold become practically accomplishable.

This DDS offers a number of unmatched advantages over existing treatment modalities. First, it requires no surgical intervention of the brain, thereby aborting risks of damaging surrounding normal tissues carrying vital brain functions. Second, the responsiveness of MION to an external magnetic field would enable a significantly enhanced active tumor targeting. Third, the low diffusivity and its endocytosis by metabolically active cells of the MION would not only provide sharper and prolonged delineation between tumor and surrounding, often edematous normal tissues, but also allow detection of (in other words, delivery of drugs to) micrometastases that often remain undetectable (due to lack of neovascularity) and at distances away from the main tumor margin. Fourth, synchronization of MRI with drug therapy would allow neuro-oncologists in staging tumors and monitoring the response to drug therapy. Lastly, owing to the non-invasiveness of this DDS, repeated or combined drug therapies can be readily carried out until the tumor volume, visualized by MRI, is reduced to a threshold value at which it can be managed by the host immune system. What's worth noting is that most of the components of the described system are feasible for clinical translation, therefore, it is envisioned that this DDS would have a great potential to effectively combat brain cancers in the foreseeable future. Last but not least, since most of technologies involved in this system can be readily applied to other DDS, the value and impact of this project in drug delivery research should be far-reaching, prevalent and wide-spread.

ACKNOWLEDGMENTS AND DISCLOSURES

This work was supported in part by National Institutes of Health R01 Grants CA114612, NS066945, and a Hartwell Foundation Biomedical Research Award. This work was also partially sponsored by Grant R31-2008-000-10103-01 from the World Class University (WCU) project of South Korea. Victor C. Yang is currently a participating faculty member in the Department of Molecular Medicine and Biopharmaceutical Sciences, Seoul National University, South Korea. It was also partially supported by National Key Basic Research Program of China (2013CB932502), School of Pharmacy, Fudan University and The Open Project Program of Key Lab of Smart Drug Delivery (Fudan University), MOE and PLA, China (SDD2011-02).

REFERENCES

1. National Cancer Institute at the U.S. National institute of health webpage. Available from: http://www.cancer.gov.
2. The children's brain tumor foundation webpage. Available from: http://www.cbtf.org/medical.b.html.
3. The brain tumor society webpage. Available from: http://www.tbts.org.
4. Grieg NH, Ries LG, Yancik R, Rapoport SI. Increasing annual incidence of primary malignant brain tumors in the elderly. J Natl Cancer Inst. 1990;82(20):1621–4.
5. Black PM. Brain tumors. New Engl J Med. 1991;324(21):1471–6.
6. Mokri B. The monro–kellie hypothesis. Neurology. 2001;56 (12):1746–8.
7. Gutman RL, Peacock G, Lu DR. Targeted drug delivery for brain cancer treatment. J Control Release. 2000;65(1–2):31–41.
8. Srinivasan R. Review of brain and brain cancer treatment. Int J Pharm Bio Sci. 2011;2(1):468–77.
9. DeAngelis LM, Delattre JY, Posner JB. Radiation-induced dementia in patients cured of brain metastases. Neurology. 1989;39 (6):789–96.
10. Nishio S, Morioka T, Fukui M. Radiation injury of the brain. Crit Rev Neurosurg. 1997;7(6):408–15.
11. New P. Radiation injury to the nervous system. Curr Opin Neurol. 2001;14(6):725–34.
12. Danoff BF, Cowchock FS, Marquette C, Mulgrew L, Kramer S. Assessment of the long-term effects of primary radiation. Therapy for brain tumors in children. Cancer. 1982;49(8):1580–6.
13. Hösli P, Sappino AP, de Tribolet N, Dietrich PY. Malignant glioma: Should chemotherapy be overthrown by experimental treatments? Ann Oncol. 1998;9(6):589–600.
14. Huynh GH, Deen DF, Szoka Jr FC. Barriers to carrier mediated drug and gene delivery to brain tumors. J Control Release. 2006;110(2):236–59.
15. Pardridge WM. Blood–brain barrier drug targeting: the future of brain drug development. Mol Interv. 2003;3(2):90–105.
16. Patel MM, Goyal BR, Bhadada SV, Bhatt JS, Amin AF. Getting into the brain: approaches to enhance brain drug delivery. Cns Drugs. 2009;23(1):35–58.
17. Rich JN, Bigner DD. Development of novel targeted therapies in the treatment of malignant glioma. Nat Rev Drug Discov. 2004;3 (5):430–46.
18. Pastan I, Chaudhary V, FitzGerald DJ. Recombinant toxins as novel therapeutic agents. Annu Rev Biochem. 1992;61(1):331–54.
19. Angelastro JM, Canoll PD, Kuo J, Weicker M, Costa A, Bruce JN, *et al.* Selective destruction of glioblastoma cells by interference with the activity or expression of atf5. Oncogene. 2005;25(6):907–16.
20. Chang L-C, Lee H-F, Yang Z, Yang V. Low molecular weight protamine (lmwp) as nontoxic heparin/low molecular weight heparin antidote (i): preparation and characterization. AAPS J. 2001;3(3):7–14.
21. Chang L-C, Liang J, Lee H-F, Lee L, Yang V. Low molecular weight protamine (lmwp) as nontoxic heparin/low molecular weight heparin antidote (ii): *in vitro* evaluation of efficacy and toxicity. AAPS J. 2001;3(3):15–23.
22. Chang L-C, Wrobleski S, Wakefield T, Lee L, Yang V. Low molecular weight protamine as nontoxic heparin/low molecular weight heparin antidote (iii): preliminary *in vivo* evaluation of efficacy and toxicity using a canine model. AAPS J. 2001;3 (3):24–31.

23. Park YJ, Chang L-C, Liang JF, Moon C, Chung C-P, Yang VC. Nontoxic membrane translocation peptide from protamine, low molecular weight protamine (lmwp), for enhanced intracellular protein delivery: *in vitro* and *in vivo* study. FASEB J. 2005;19 (11):1555–7.
24. Byun Y, Singh VK, Yang VC. Low molecular weight protamine: a potential nontoxic heparin antagonist. Thromb Res. 1999;94 (1):53–61.
25. Liang JF, Zhen L, Chang LC, Yang VC. A less toxic heparin antagonist—low molecular weight protamine. Biochem Mosc. 2003;68(1):116–20.
26. Fawell S, Seery J, Daikh Y, Moore C, Chen LL, Pepinsky B, *et al.* Tat-mediated delivery of heterologous proteins into cells. Proc Natl Acad Sci. 1994;91(2):664–8.
27. Suzuki T, Futaki S, Niwa M, Tanaka S, Ueda K, Sugiura Y. Possible existence of common internalization mechanisms among arginine-rich peptides. J Biol Chem. 2002;277(4):2437–43.
28. Chertok B, David AE, Yang VC. Brain tumor targeting of magnetic nanoparticles for potential drug delivery: effect of administration route and magnetic field topography. J Control Release. 2011;155(3):393–9.
29. Protamine sulfate. In: Ahfs drug information. Bethesda: American Hospital Formulary Service; 2001. p. 1408–9.
30. Kwon YM, Li Y, Naik S, Liang JF, Huang Y, Park YJ, *et al.* The attempts delivery systems for macromolecular drugs. Expert Opin Drug Deliv. 2008;5(11):1255–66.
31. Strausbaugh LJ. Intracarotid infusions of protamine sulfate disrupt the blood–brain barrier of rabbits. Brain Res. 1987;409(2):221–6.
32. Chertok B, Moffat BA, David AE, Yu F, Bergemann C, Ross BD, *et al.* Iron oxide nanoparticles as a drug delivery vehicle for mri monitored magnetic targeting of brain tumors. Biomaterials. 2008;29(4):487–96.
33. Lee Y, Mo H, Koo H, Park J-Y, Cho MY, Jin G-w, *et al.* Visualization of the degradation of a disulfide polymer, linear poly(ethylenimine sulfide), for gene delivery. Bioconjug Chem. 2006;18(1):13–8.
34. Oupický D, Parker AL, Seymour LW. Laterally stabilized complexes of DNA with linear reducible polycations: strategy for triggered intracellular activation of DNA delivery vectors. J Am Chem Soc. 2001;124(1):8–9.
35. Reddy GR, Bhojani MS, McConville P, Moody J, Moffat BA, Hall DE, *et al.* Vascular targeted nanoparticles for imaging and treatment of brain tumors. Clin Cancer Res. 2006;12 (22):6677–86.
36. Chertok B, David AE, Yang VC. Delivery of functional proteins to brain tumor using mri-monitored, magnetically-targeted nanoparticles. J Control Release. 2008;132(3):e61–2.
37. Gamarra LF, Pontuschka WM, Amaro Jr E, Costa-Filho AJ, Brito GES, Vieira ED, *et al.* Kinetics of elimination and distribution in blood and liver of biocompatible ferrofluids based on fe3o4 nanoparticles: an epr and xrf study. Mater Sci Eng C Bio Syst. 2008;28 (4):519–25.
38. Ślawska-Waniewska A, Mosiniewicz-Szablewska E, Nedelko N, Gałązka-Friedman J, Friedman A. Magnetic studies of iron-entities in human tissues. J Magn Magn Mater. 2004;272–6. Part 3(0):2417–2419.
39. Chertok B, Cole AJ, David AE, Yang VC. Comparison of electron spin resonance spectroscopy and inductively-coupled plasma optical emission spectroscopy for biodistribution analysis of iron-oxide nanoparticles. Mol Pharm. 2010;7(2):375–85.
40. Enochs WS, Harsh G, Hochberg F, Weissleder R. Improved delineation of human brain tumors on mr images using a long-circulating, superparamagnetic iron oxide agent. J Magn Reson Imaging. 1999;9(2):228–32.
41. Kim T, Shima M. Reduced magnetization in magnetic oxide nanoparticles. J Appl Phys. 2007;101(9):09M516.
42. Papisov MI, Bogdanov Jr A, Schaffer B, Nossiff N, Shen T, Weissleder R, *et al.* Colloidal magnetic resonance contrast agents: effect of particle surface on biodistribution. J Magn Magn Mater. 1993;122(1–3):383–6.
43. Lübbe AS, Bergemann C, Huhnt W, Fricke T, Riess H, Brock JW, *et al.* Preclinical experiences with magnetic drug targeting: tolerance and efficacy. Cancer Res. 1996;56 (20):4694–701.
44. Yoshizaki K, Adachi K, Kataoka S, Watanabe A, Tabira T, Takahashi K, *et al.* Chronic cerebral hypoperfusion induced by right unilateral common carotid artery occlusion causes delayed white matter lesions and cognitive impairment in adult mice. Exp Neurol. 2008;210(2):585–91.
45. Driscoll CF, Morris RM, Senyei AE, Widder KJ, Heller GS. Magnetic targeting of microspheres in blood flow. Microvasc Res. 1984;27(3):353–69.
46. Chertok B, David AE, Yang VC. Magnetically-enabled and mr-monitored selective brain tumor protein delivery in rats via magnetic nanocarriers. Biomaterials. 2011;32(26):6245–53.
47. Chertok B, David AE, Yang VC. Polyethyleneimine-modified iron oxide nanoparticles for brain tumor drug delivery using magnetic targeting and intra-carotid administration. Biomaterials. 2010;31 (24):6317–24.
48. Pulfer SK, Gallo JM. Enhanced brain tumor selectivity of cationic magnetic polysaccharide microspheres. J Drug Target. 1998;6 (3):215–27.
49. Thorpe PE, Burrows FJ. Antibody-directed targeting of the vasculature of solid tumors. Breast Cancer Res Treat. 1995;36(2):237–51.
50. Bandres E, Andion E, Escalada A, Honorato B, Catalan V, Cubedo E, *et al.* Gene expression profile induced by bcnu in human glioma cell lines with differential mgmt expression. J Neuro-Oncol. 2005;73(3):189–98.
51. McNeil PL, Murphy RF, Lanni F, Taylor DL. A method for incorporating macromolecules into adherent cells. J Cell Biol. 1984;98(4):1556–64.
52. Chakrabarti R, Wylie DE, Schuster SM. Transfer of monoclonal antibodies into mammalian cells by electroporation. J Biol Chem. 1989;264(26):15494–500.
53. Basu SK. Receptor-mediated endocytosis of macromolecular conjugates in selective drug delivery. Biochem Pharmacol. 1990;40(9):1941–6.
54. Schwarze SR, Ho A, Vocero-Akbani A, Dowdy SF. *In vivo* protein transduction: delivery of a biologically active protein into the mouse. Science. 1999;285(5433):1569–72.
55. Huang Y, Shin Park Y, Wang J, Moon C, Min Kwon Y, Sun Chung H, *et al.* Attempts system: a macromolecular prodrug strategy for cancer drug delivery. Curr Pharm Des. 2010;16(21):2369–76.
56. Bagshawe KD. Antibody directed enzymes revive anti-cancer prodrugs concept. Brit J Cancer. 1987;56(5):531–2.
57. Syrigos KN, Epenetos AA. Antibody directed enzyme prodrug therapy (adept): a review of the experimental and clinical considerations. Anticancer Res. 1999;19(1A):605–13.
58. Liang JF, Li YT, Song H, Park YJ, Naik SS, Yang VC. Attempts: a heparin/protamine-based delivery system for enzyme drugs. J Control Release. 2002;78(1–3):67–79.
59. Doxorubicin hydrochloride. In: Ahfs drug information. Bethesda: American Hospital Formulary Service; 2001. p. 950–60.
60. Asparaginase. In: Ahfs drug information. Bethesda: American Hospital Formulary Service; 2001. p. 872–5.
61. Niesner U, Halin C, Lozzi L, Günthert M, Neri P, Wunderli-Allenspach H, *et al.* Quantitation of the tumor-targeting properties of antibody fragments conjugated to cell-permeating hiv-1 tat peptides. Bioconjug Chem. 2002;13(4):729–36.

62. Pulfer SK, Ciccotto SL, Gallo JM. Distribution of small magnetic particles in brain tumor-bearing rats. J Neuro-Oncol. 1999;41(2):99–105.
63. McBain SC, Yiu HHP, El Haj A, Dobson J. Polyethyleneimine functionalized iron oxide nanoparticles as agents for DNA delivery and transfection. J Mater Chem. 2007;17(24):2561–5.
64. Park YJ, Liang JF, Ko KS, Kim SW, Yang VC. Low molecular weight protamine as an efficient and nontoxic gene carrier: *in vitro* study. J Gene Med. 2003;5(8):700–11.
65. Futami J, Kitazoe M, Maeda T, Nukui E, Sakaguchi M, Kosaka J, *et al.* Intracellular delivery of proteins into mammalian living cells by polyethylenimine-cationization. J Biosci Bioeng. 2005;99(2):95–103.
66. Stivaktakis N, Nikou K, Panagi Z, Beletsi A, Leondiadis L, Avgoustakis K. Immune responses in mice of β-galactosidase adsorbed or encapsulated in poly(lactic acid) and poly(lactic-co-glycolic acid) microspheres. J Biomed Mater Res A. 2005;73A(3):332–8.
67. Alexiou C, Arnold W, Klein RJ, Parak FG, Hulin P, Bergemann C, *et al.* Locoregional cancer treatment with magnetic drug targeting. Cancer Res. 2000;60(23):6641–8.
68. Weissleder R, Stark DD, Engelstad BL, Bacon BR, Compton CC, White DL, *et al.* Superparamagnetic iron oxide: pharmacokinetics and toxicity. Am J Roentgenol. 1989;152(1):167–73.
69. Eckman WW, Patlak CS, Fenstermacher JD. A critical evaluation of the principles governing the advantages of intra-arterial infusions. J Pharmacokinet Biopharm. 1974;2(3):257–85.